

Original Study

Open Access

Adrian Błonka*, Łukasz Skrzętkowicz

Nonlinear buckling analysis of network arch bridges

<https://doi.org/10.2478/sgem-2022-0007>

received October 2, 2021; accepted January 11, 2022.

Abstract: The paper presents designing due to the instability in-plane problem of the net-arch bridge. Firstly, three essential nonlinear examples are benchmarked in a finite element software. Secondly, linear and nonlinear buckling analyses are conducted, with the purpose of investigating the impact of nonlinear behavior of cables on steel arch instability, involving a comparison of the critical load factor and form from both the linear buckling and the post-critical third-order theory analyses. The impact of prestress and tension, elevation, and hanger failure on instability is discussed. Moreover, a new method for determining nonlinear buckling form for the net-arch structure is proposed in order to allow implementation of Unique Global and Local Imperfection method in cable structures. Calculations are conducted in the finite element software. The model of the network arch bridge is based on the bridge over Vistula River in Cracow.

Keywords: Network arch bridge; post-critical analysis; nonlinear buckling; unique global and local imperfection form; cable structures.

1 Introduction

First net-arch bridge was proposed by Tveit [8-14], who, at the same time, proposed the usage of an open H-section in the construction of a steel arch as an alternative for the commonly used welded rectangular or circular boxes. These structures are highly efficient in the middle span road and train bridge solutions and are more and more frequently used in the bridge industry. Hangers are made of tensioned cables, and their distribution is radial. Ties

are usually constructed as the orthotropic steel deck or the longitudinal prestressed concrete deck (sometimes both longitudinal and perpendicular) because of high tension. In the design process, the stability of steel arch is the key issue. Mostly, linear buckling analysis (LBA) is conducted in the finite elements analysis (FEA) software [2, 4, 5]. Alternatively, the solution for beam supported by flexible springs is used as a first estimation, especially in optimization tasks, due to its simplicity. Both of them are based on linear analysis. In a structure with slender elements, geometrical nonlinear effects could be significant, causing reduction of the arch buckling resistance. In accordance with the general method for lateral and lateral torsional buckling of structures [17], stability could be analyzed in two ways, the so-called in plane and out of plane. The out-of-plane stability of the arch could be considered similarly as a swayed frame. Since hangers are perpendicular to possible out-of-plane displacements, the impact of cables is negligible. The in-plane stability could be taken into account by various methods. One of the most convenient application methods is the procedure described in Eurocode 3 [17], Unique Global and Local Imperfection (UGLI), which contains the most unfavorable combination of sway and bow imperfections. This method requires to obtain the real buckling form and the corresponding critical load factor. This buckling form is influenced by the nonlinear behavior of cable elements (reduction of stiffness caused by the sag), and as a result, the critical load factor could be misestimated when only linear analysis is performed. In this paper, differences between LBA and non-LBA in different design situations are investigated.

2 Principal examples

2.1 Types of Analyses

In the geometrical nonlinear analysis (GNA), the correlations between applied force and displacement of nodes are described by equilibrium path [6, 16]. This path is mostly described by a curve. Two types of specific points can manifest on this path: the bifurcation point

*Corresponding author: Adrian Błonka, Wrocław University of Science and Technology, Doctoral School, Faculty of Civil Engineering, Discipline of Civil Engineering and Transport, Department of Structural Mechanics and Urban Engineering, Wrocław, Poland, E-mail: adrian.blonka@gmail.com, Łukasz Skrzętkowicz, Wrocław University of Science and Technology, Faculty of Civil Engineering, Department of Building Structures, Wrocław, Poland

and the limit point. The bifurcation point is a result of an intersection between different equilibrium paths (mostly two). These paths can be both stable and unstable, changing state after crossing this point (Fig. 1). If the path changes from stable to unstable state and no other path intersects at this point, then limit point occurs. The load factor for the limit point can be both lesser and greater than the load factor for the bifurcation point. Bifurcation point is mostly related to the LBA or second-order theory (TH2) analysis. The limit point cannot be obtained by LBA and TH2 analysis, even if the load factor value for the limit point is lesser than value of the load factor for the bifurcation point. Only third-order theory (TH3) analysis provides this possibility. It is based on non-simplified curvature equation and provides more accurate results for large deflections, mostly applicable for slender elements, for instance, cables. After reaching the limit point, the structure resistance decreases until the next limit is reached (Fig. 2). Then, the resistance starts rising and can reach the same load factor as for the first limit point. This phenomenon is called the snap instability and two major categories are highlighted. The snap-back occurs when deflections on the equilibrium path decline between the first and second limit points and then grow. The snap-through occurs when deflections keep growing after reaching the first limit point (Fig. 2). The snap-back instability is characteristic for thin plates in silos and tanks, and the snap-through instability is typical for structures with low elevation. Possibly, the bifurcation point can transform to the limit point when an imperfected structure is considered (Fig. 2).

The nonlinear phenomena are solved to illustrate possibilities of different types of numerical analyses. All calculations are performed in a SOFiSTiK FEA program. The software is benchmarked by comparing results from three examples to solutions from the technical literature. The von Mises truss is taken into consideration as the general overview. A compressed column and a bending beam, both with bow imperfections, are considered as a direct reference to a possible net-arch behavior.

2.2 Geometrically nonlinear phenomenon – von Mises truss

The von Mises truss is a symmetrical beam structure, widely used as an example of snap-through instability phenomenon. This model is made of two beams with low elevation. Connections are made of hinges. Supports are pinned. An initial point load of 1 kN or 1 mm is attached to a keystone. The cross section of beams is IPE 100, the total span is 2.0 m, and elevation is 0.1 m (Fig. 3).

Firstly, LBA is conducted for the nondeformed structure. The resultant critical load factor value corresponds exactly with the critical load value. Secondly, the TH3 analysis is conducted. The stiffness matrix is updated every step by increasing the load factor or the displacement. This task is convergent in the unstable path fragment, and the residual forces are negligible.

Load factors for force and displacement loads are different because of the various behaviors of these loads. The vertical reaction forces are read for the same point of reference. Results match exactly for the FEA program with the TH3 analysis and the displacement load and for the equilibrium path from the analytical solution. In the case of force load, instead of the displacement load, results match the analytical solution likewise, and snap-through path occurs after the first limit point (Fig. 4). The difference is significant between forms (Fig. 5) from buckling analysis and TH3 analysis (when the structure returns to the stable path part after reaching the first limit point). The load factor is 462.2 for the bifurcation point and 82.5 for the limit point. This phenomenon shows the importance of the GNA application.

2.3 Imperfected column

Two crucial internal forces in net-arch structures are compressing normal forces and in-plane bending moments. The imperfected column is considered for benchmarking an influence of normal forces. Two lengths ($L = 40$ m, $L = 100$ m) of the arch with six elevations ($L/300$, $L/200$, $L/100$, $L/30$, $L/20$, $L/10$) are considered, 12 cases in total. The column has an IPE 100 prismatic cross section and is divided into 400 beam elements. The point load is applied in a roller support and remains stationary. Supports along the column are applied to prevent out-of-plane buckling forms (Fig. 6).

The LBA, TH2, and TH3 analyses are conducted. The LBA and TH2 analysis provide almost the same bifurcation critical load factor with maximum divergency of 1.4% in the considered range, whereby the TH2 equilibrium path reaches it asymptotically, as expected (Fig. 7 a, b). In the TH3 analysis, the critical load factor exceeds the bifurcation point asymptote and then increases gradually (Fig. 7 c). Values of the critical load factor drop rapidly after reaching the limit point and then start to increase again. The limit point is correlated with the twist of the column. In this case, the bifurcation point does not occur on the TH3 equilibrium path, so consequently, LBA should be processed because of the possibility of the lesser buckling load factor than the limit point factor.

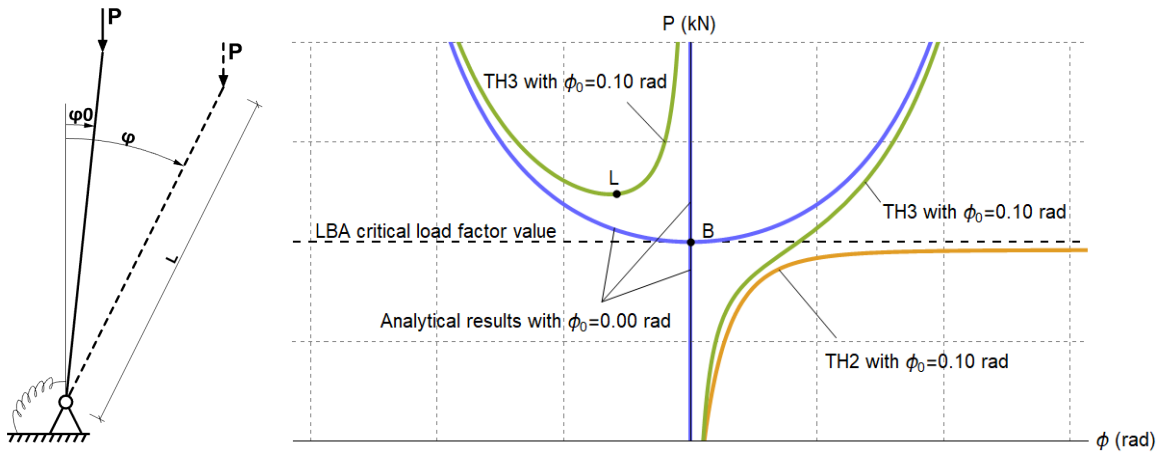


Figure 1: Comparison of sample equilibrium paths for different types of analyses (B – bifurcation point, L – limit point).

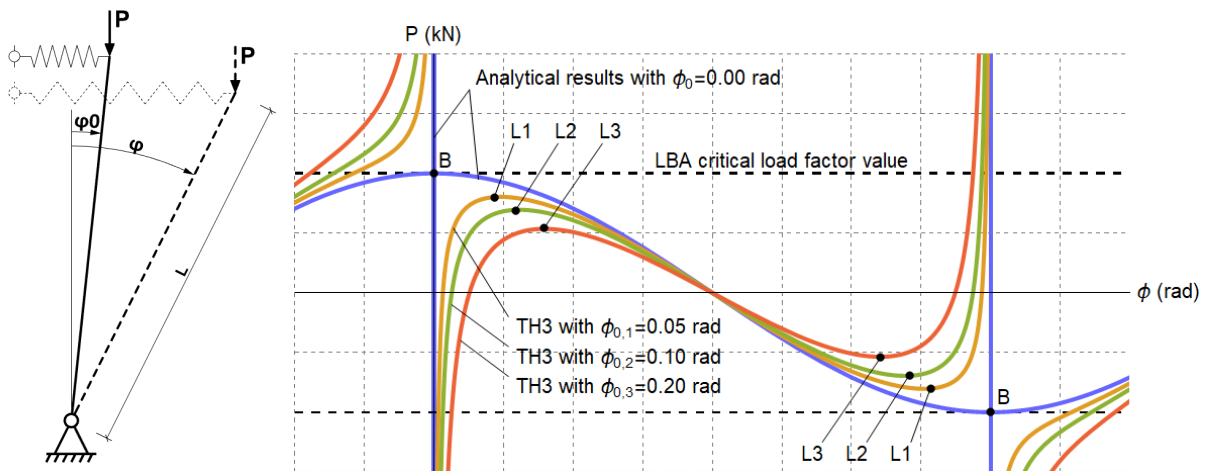


Figure 2: Comparison of sample equilibrium paths with the snap-through instability (B – bifurcation point, L – limit point).

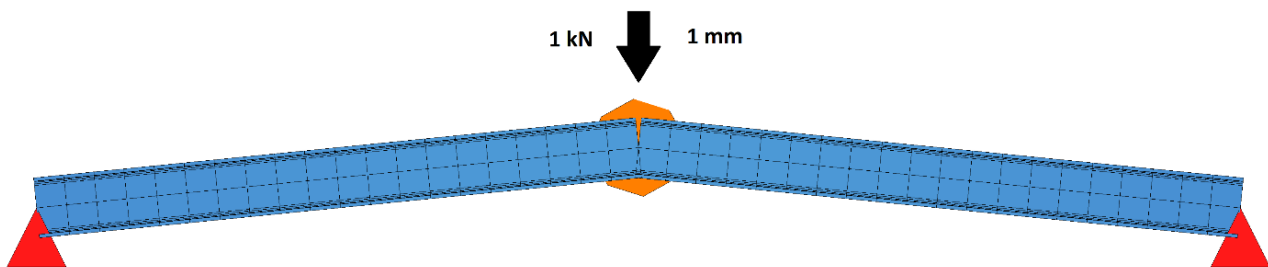


Figure 3: The model of von Mises truss.

2.4 Imperfected beam

This example is considered for benchmarking the instability caused by the bending load. The beam has 120 m length, 12 m elevation, HD 400 x 990 prismatic cross section, and is divided into 400 beam elements.

Supports are pinned. Supports along the beam are used for preventing out-of-plane buckling forms. Uniform and point loads are considered for application on each beam and node (Fig. 8).

The LBA and TH3 with postcritical analysis are conducted.

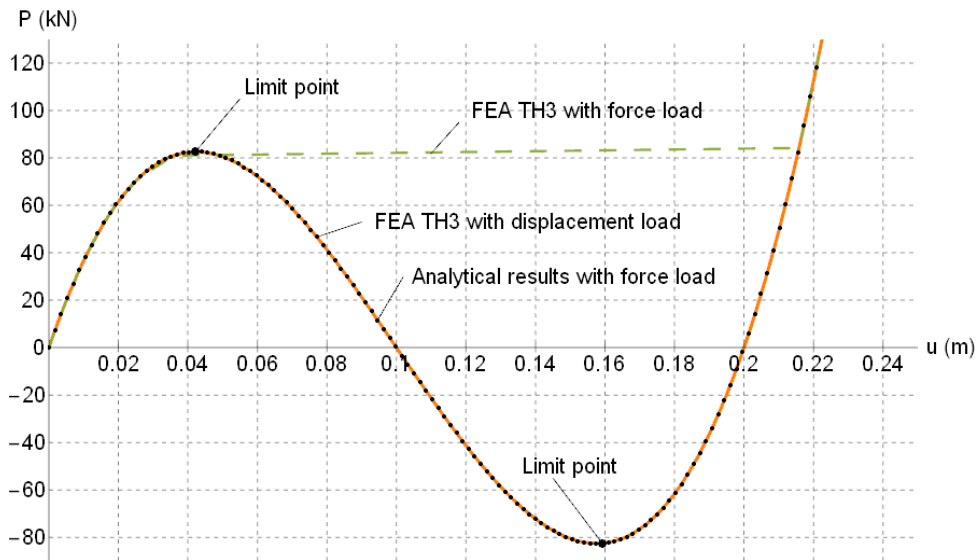


Figure 4: Equilibrium paths for von Mises truss from different types of analysis. The vertical axis represents applied force and the horizontal axis represents the displacement of the point where the load is applied. FEA TH3 with displacement results (continuous) match exactly the analytical results with force load (dotted).

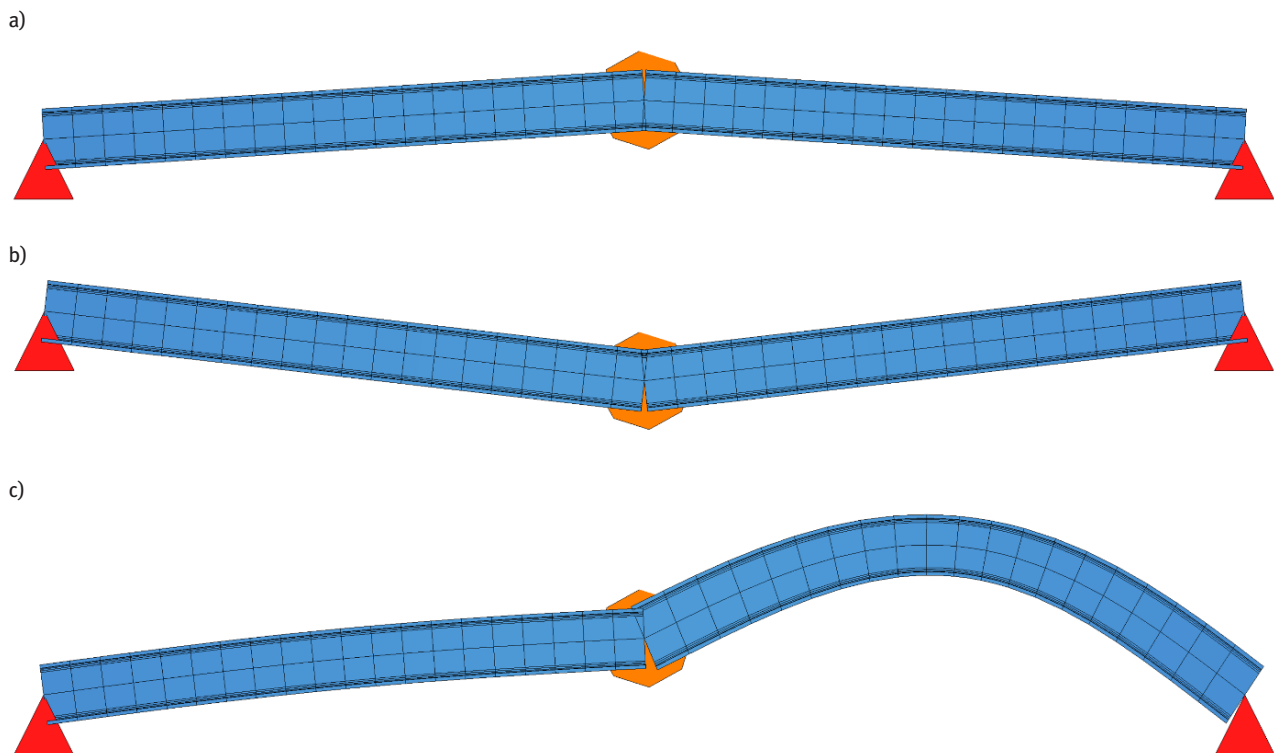


Figure 5: Instability forms: (a) structure without deformation, (b) form after snap-through, (c) first buckling form.

The instability form should not take into consideration deformations caused by loading before reaching the limit point. Deformations are considered in the UGLI method during the design process. The deformations are subtracted from the postcritical form, so displacements from the

postcritical 3rd order theory analysis, so-called PUSH procedure in SOFiStiK, are reduced by displacements from the last stable state form. The displacement progression is presented in Fig. 9, and plots are scaled with different factors for comparison. The form after approximately 20

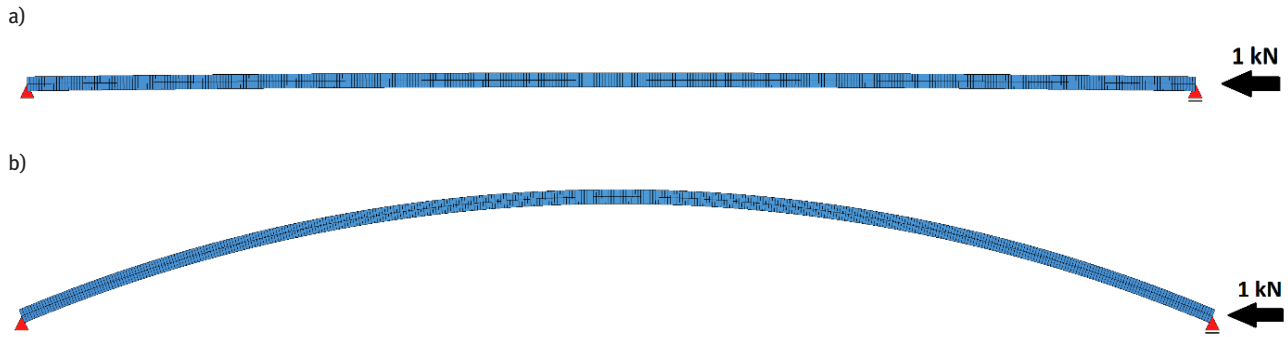


Figure 6: Sample geometry of columns with the lowest (a) and highest (b) elevation with initial loads.

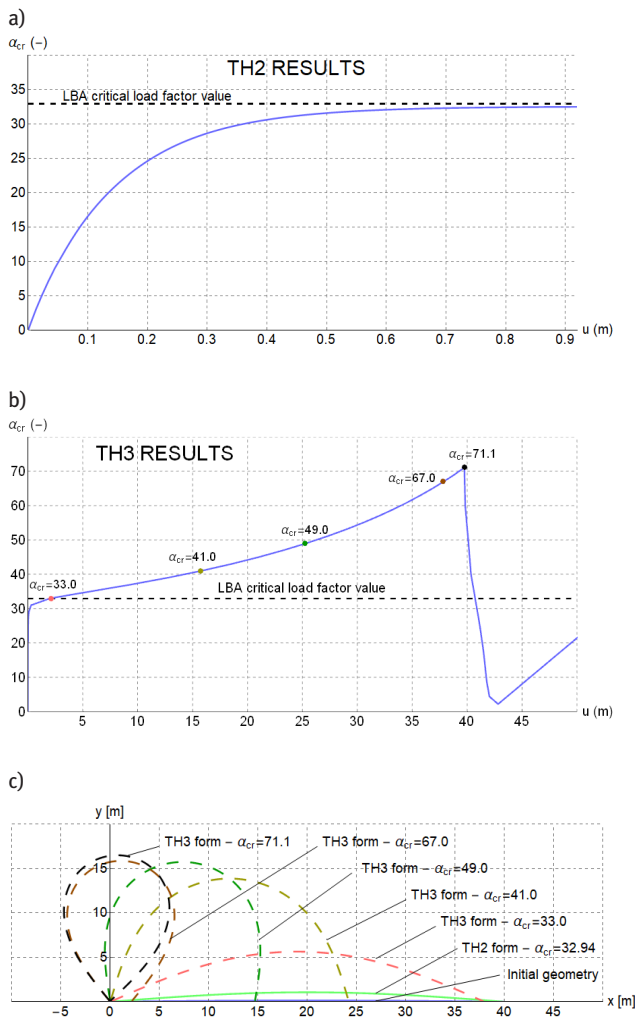


Figure 7: Midpoint equilibrium paths for TH2 (a) and TH3 (b) analyses and corresponding displacements (c) of 40-m-long column with a 1/300 elevation (equivalent imperfection $e_0 = 0.133$ m).

pushes matches thoroughly with the buckling form. The load factor for the limit point is close to the bifurcation point value with a maximum error of 2.0%.

3 Task Parameters

3.1 Geometry and material

Since this task focuses on the in-plane stability of the net-arch, the calculations are performed for single arch prevented from out-of-plane buckling (both flexural and lateral-torsional). The geometry of the arch is adapted from the longest bridge over Vistula River in Cracow [3]. The bridge is the first railway network arch bridge constructed from cold-bent HD sections and composite dowels [7].

A new type of composite element located in a skewback was proposed by Sęk and Lorenc [7] (Fig. 10). This double composite section increases the rigidity of the portal frame and enables a smooth transition from the arch steel into a longitudinally prestressed concrete deck. Additionally, this part increases the in-plane stability by stiffening the arch ends and reduces the necessity of hangers in the ends.

The simplified planar model has a length of 116 m and an elevation of 17.4 m (Fig. 11, 12). A heavy H-section HD 400 x 1299 made of structural steel S460 HISTAR is used for arch beam elements. The section starts extending to 12-m distance from skewbacks. The linear extension occurs in height from standard dimension to 1520 mm. Skewbacks are made of the concrete C55/67 and are modeled by 1.20-m-thick shell elements. The tie-deck is assumed as a beam element with rectangular 600 x 7000 mm cross section. The deck width is estimated as half of the original bridge. No load eccentricities are considered. Hangers are distributed radially, with spacing ranging between 1.3 and 2.7 m along the arch curvature, 44 in total. They are modeled as cable elements with no compressive stiffness and divided into five parts. The angle of inclination changes gradually from 30° to 75°. The cross section is circular with 87 mm in diameter .

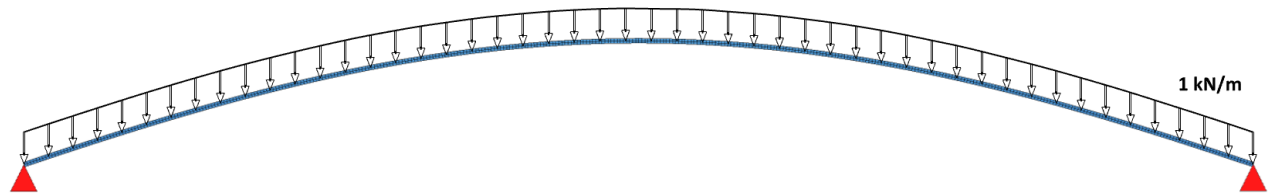


Figure 8: The geometry of the beam with initial uniform loads.

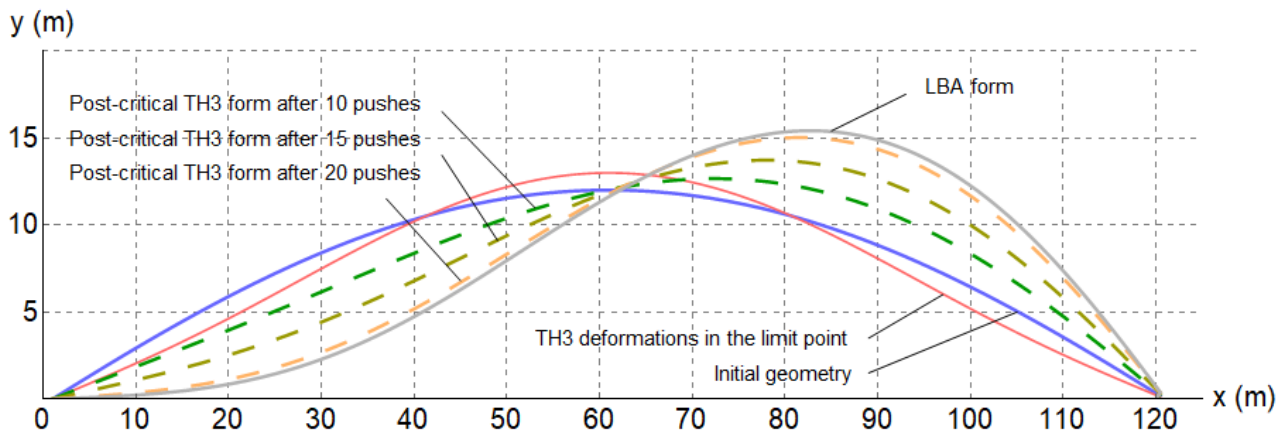


Figure 9: Scaled deformation forms from buckling and TH3 analysis.



Figure 10: Photos of network arch bridge over Vistula River in Cracow (own source).

3.2 Calculation methods

All calculations are performed in the SOFiStiK software. Firstly, as the most exact one, the TH3 analysis is conducted for all types of elements. It provides a possibility for taking into account reduced stiffness of sagged hangers when deformation occurs, which is omitted in the LBA. The program used offers combinational analysis including the TH3 for cable elements and the TH2 for beams, the so-called TH3B, and possibly shortens the calculation time without affecting accuracy of the results, if beam-

related geometrical nonlinear effects are negligible. TH2 is omitted because of the low accuracy for cable elements. The critical load value is obtained by increasing the load factor stepwise, so-called ULTI procedure in SOFiStiK. Thereafter, the post-critical analysis is controlled by a deformation increment in a procedure called PUSH. Depending on results, the load factor is adapted and can also decrease. Finally, the LBA is performed. All procedures are conducted with material linearity.

The modified train load model LM71 is considered (Fig. 13). An uniformly distributed load is applied along

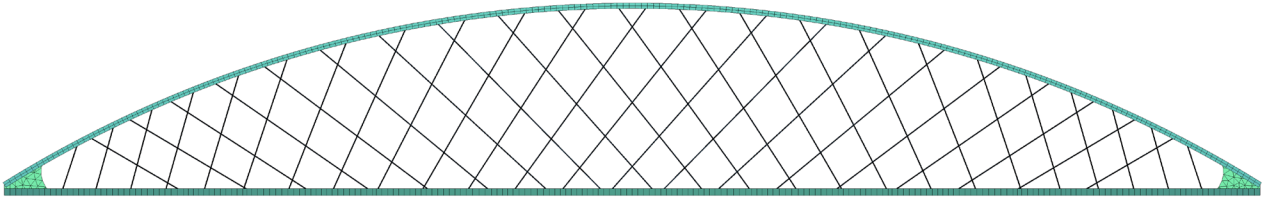


Figure 11: Side view of the numerical model.

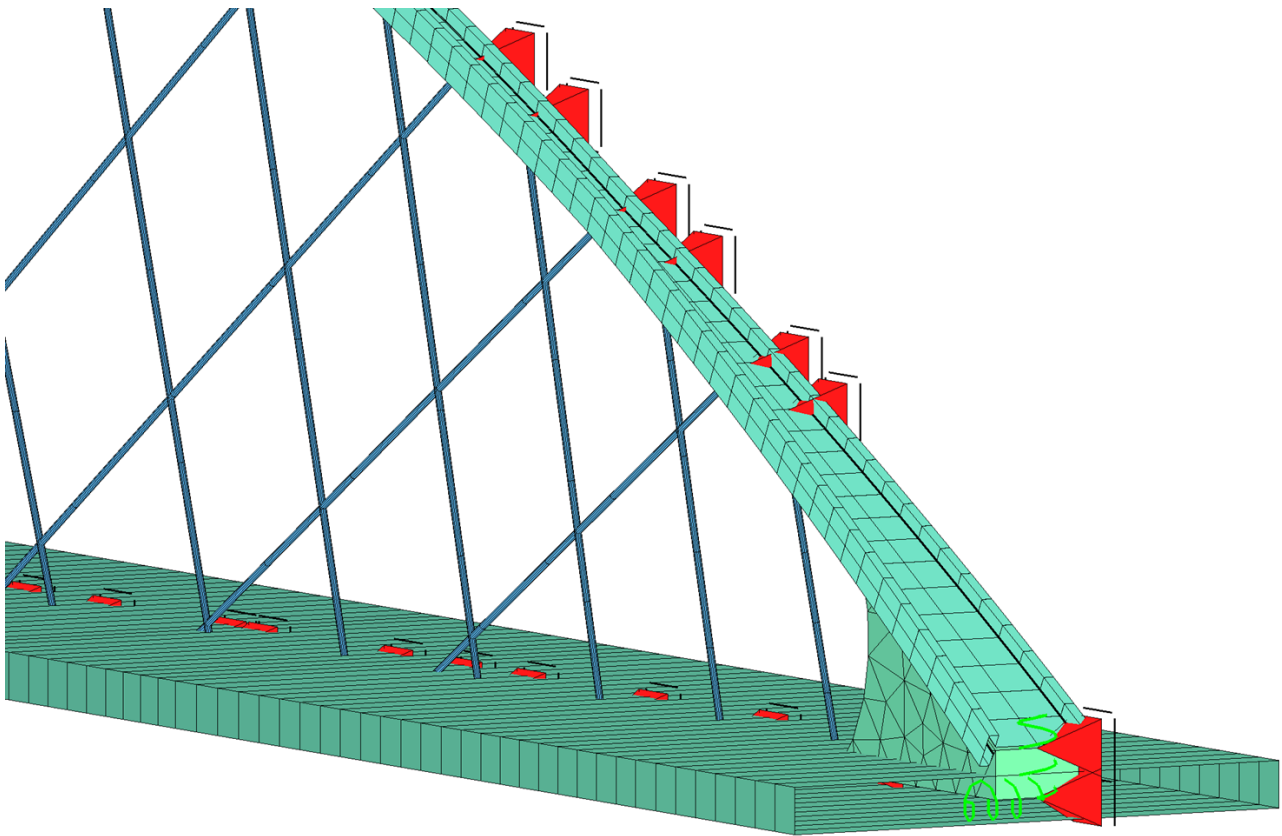


Figure 12: Detail view of the skewback.

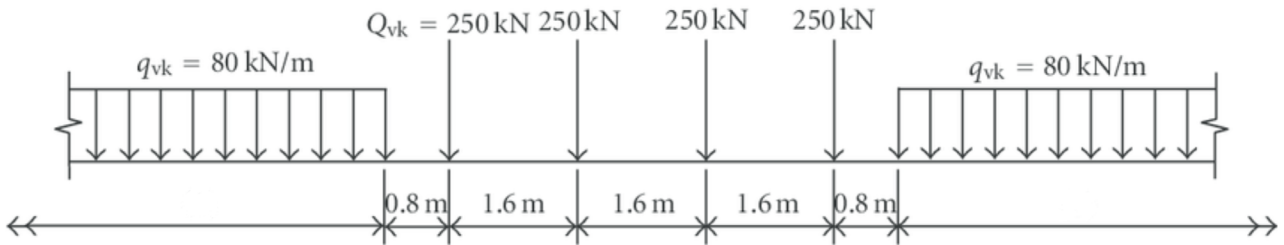


Figure 13: Load Model 71 and characteristic value for vertical load from Eurocode [19].

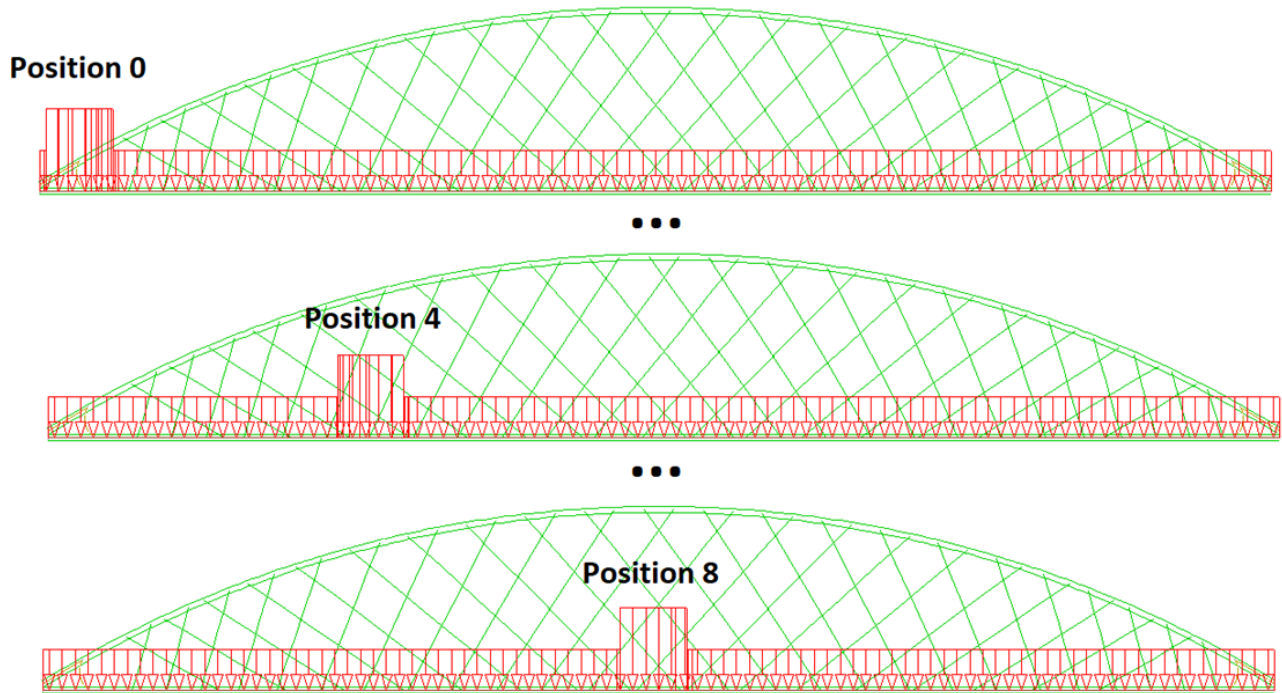


Figure 14: The LM 71 positions along the span.

the span with a value of 80 kN/m, and an additional uniformly distributed load of 80 kN/m is applied segmentally along the span with length of each segment equal to 6,4 m (Fig. 14). Nine positions of live loads, from skewback to midspan, are considered. A deadload is always taken into account (deadload-to-live load ratio is about 1.4). Prestressing of tie-deck and tension of hangers are applied depending on the performed analysis.

4 Results

4.1 Influence of prestress and tension

The impact of longitudinal prestressing in the tie-deck and tensioning of the hangers on the arch's stability is analyzed. Longitudinal prestressing is used in the network arch bridges to prevent the deck from cracking. Three values of hangers' tensioning (1, 500, and 1000 kN) and three values of deck's prestressing (10, 15, and 20 MN) are considered and results are compared to the base state (when prestress and tension do not occur), 10 cases in total. Nine positions of the live load are considered for every case. The critical load factor, α_{cr} , one of the most significant measures by which loads have to be increased to cause elastic instability in a global mode (in plane in this case), is obtained from

the LBA and the ULTI procedure. As mentioned before, cable structures may be sensitive for geometrical nonlinear effects and this may affect the buckling resistance. In order to analyze this impact, the geometrical nonlinear-to-linear critical load factor ratio is calculated (Fig. 15). Furthermore, buckling forms from the LBA and TH3 analysis are compared (Figs 16 and 17). According to principal example of the bending beam, deformations from the PUSH analysis are reduced by deformations from the last stable state (last ULTI step) to avoid precritical deflections (Fig. 17). A length of each PUSH step is equal to 5% of the maximum deformation from the limit point.

In the considered examples, the critical load factor from the LBA is unaffected by tension and prestress. This factor decreases modestly from 9.2 to 8.8 when the load is closer to the middle of the bridge length. The critical load factor obtained in the ULTI procedure changes in a wider range from 7.5 to 8.7 and generally declines when the load moves toward midspan (Fig. 15). The critical load factor ratios for low tensioning and for all prestress cases are almost the same as for the case, when prestressing and tensioning do not occur. When tensions get higher, the ratios get lower, and still prestressing has a negligible effect on the ratios' value. For middle and high tension (MT and HT), the ratios drop by 5% and 7.5%–10%, respectively, in comparison with low tension (LT). In all considered

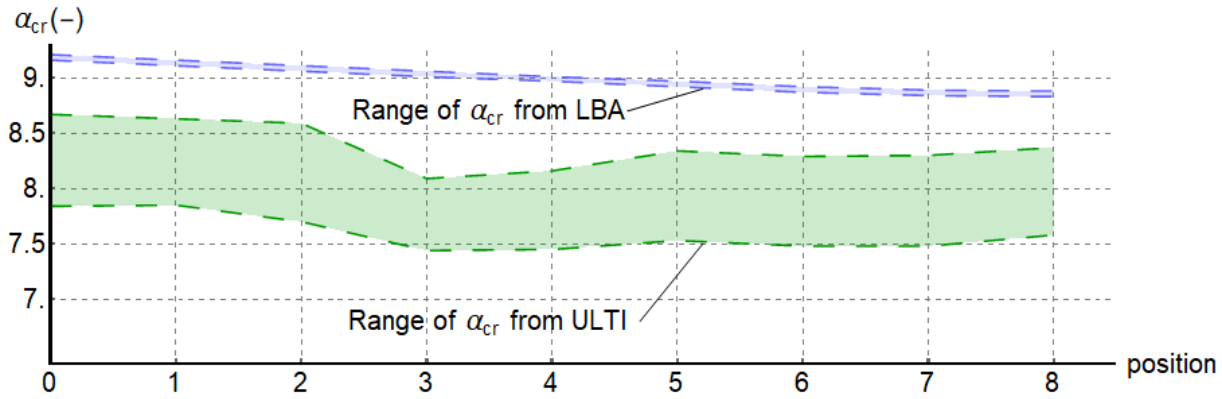


Figure 15: Resultant ranges of the critical load factors for the LBA and ULTI analysis.

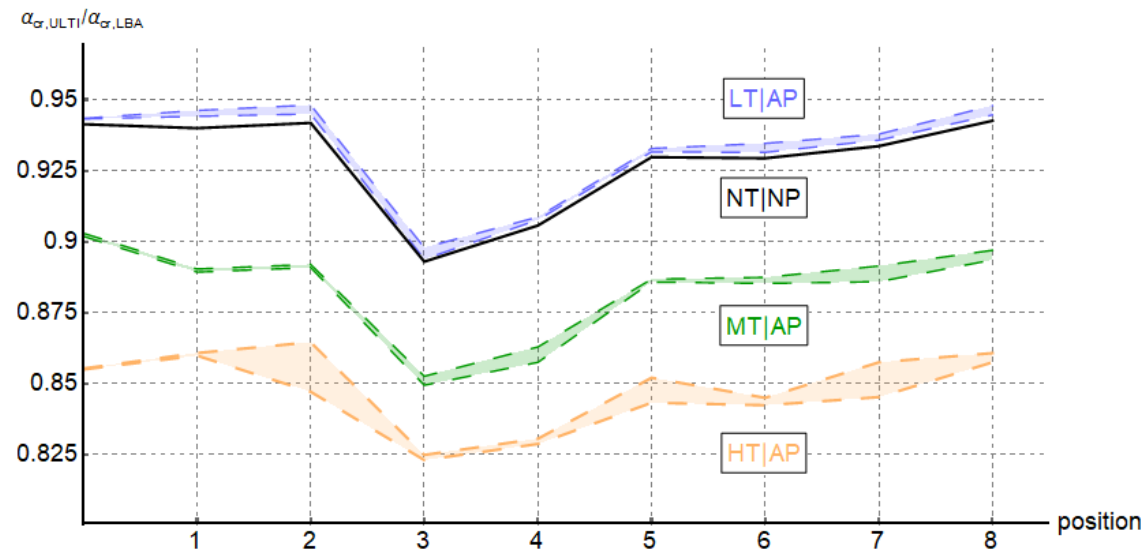


Figure 16: Resultant ranges of critical load factor ratios. NT – no tension, LT – low tension (1 kN), MT – middle tension (500 kN), HT – high tension (1000 kN), NP – no prestress, AP – all prestress cases (10, 15, 20 MN).

situations, a significant drop in the ratios' values can be noticed when loads are applied in approximately one-fourth of the span length. This tendency is correlated with the most unfavorable load case position for arches.

The stability forms from LBA and TH3 analysis are scaled with the same deformation amplitude. Buckling forms oscillate along the arch and all of them are similar, because change of displacement is relatively negligible. On the other hand, the shapes of TH3's forms are similar in trends and fluctuations to buckling forms; however, additional displacements appear nearby skewback. Moreover, deflections occur more frequently beneath than above the arch axis, which suggests that additional bow imperfections are included, in spite of reducing displacement from the PUSH analysis by the ULTI

procedure. Furthermore, the change of range of possible displacements from TH3 analysis is greater than from LBA. The possible range of displacements for nonlinear forms rises in cables with big sag, which results in stiffness reduction. This phenomenon cannot be taken into account in LBA.

4.2 Influence of elevation

The influence of various elevations (0.12, 0.14, 0.15, 0.16, and 0.18 fraction of the span length) of the arch is analyzed with no tension and no prestress. Nine load cases of live load are considered for every elevation. Results and trends are presented in Fig. 18.

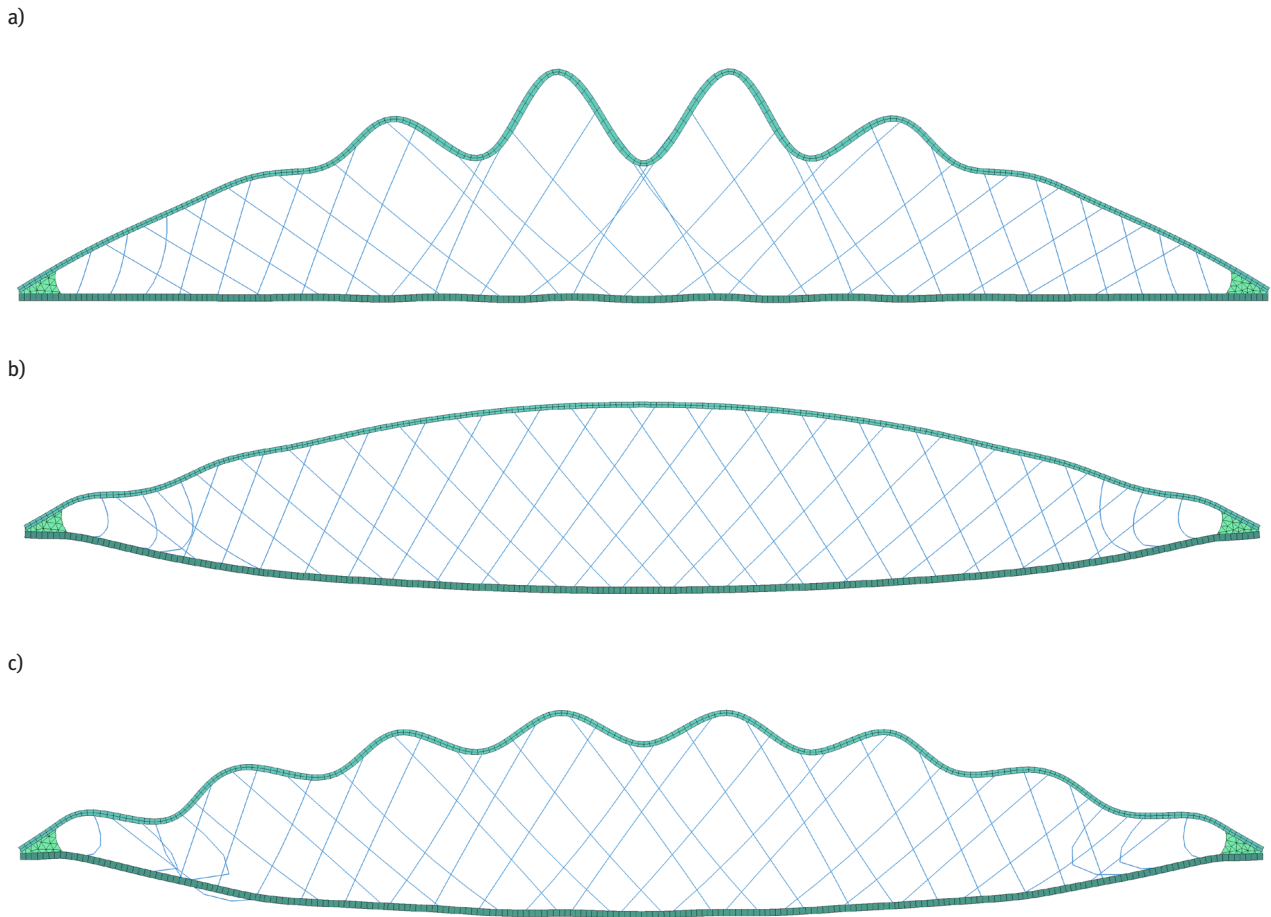


Figure 17: Deformations form: LBA (a), last ULTI step (b), and PUSH after 50 steps (c).

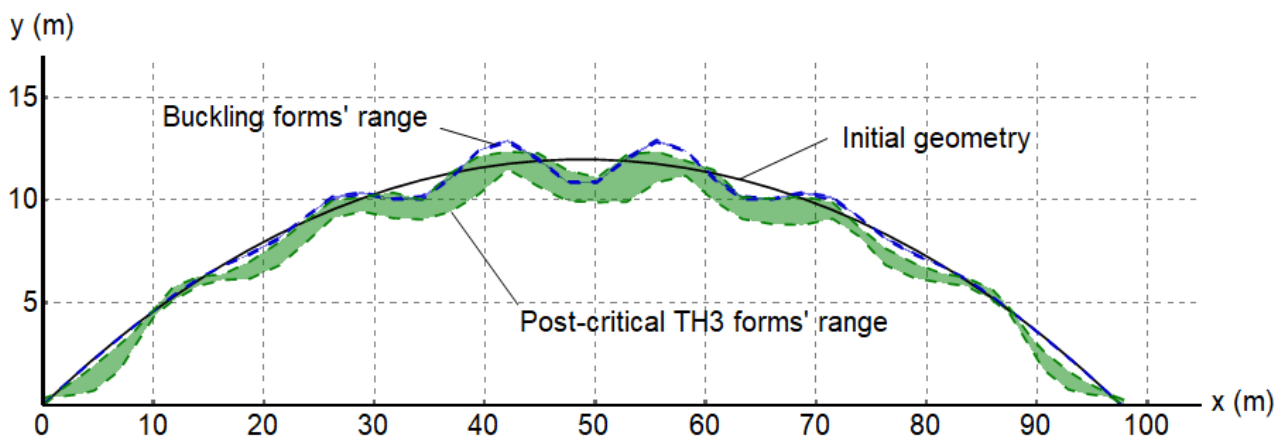


Figure 18: Scaled deformation forms of the arch between skewbacks from LBA and TH3 analysis.

The differences in ULTI-to-LBA critical load factor ratios for the highest and the lowest considered elevation are mostly less than 1%, especially in comparison to the referenced 0.15 elevation; therefore, elevation has a slight impact on the critical load ratios in a reasonable range of values.

4.3 Accidental state

In this case, impact on the arch instability in an accidental state, when hangers are ruptured, is analyzed through critical load factor ratios and instability forms. Rupture of

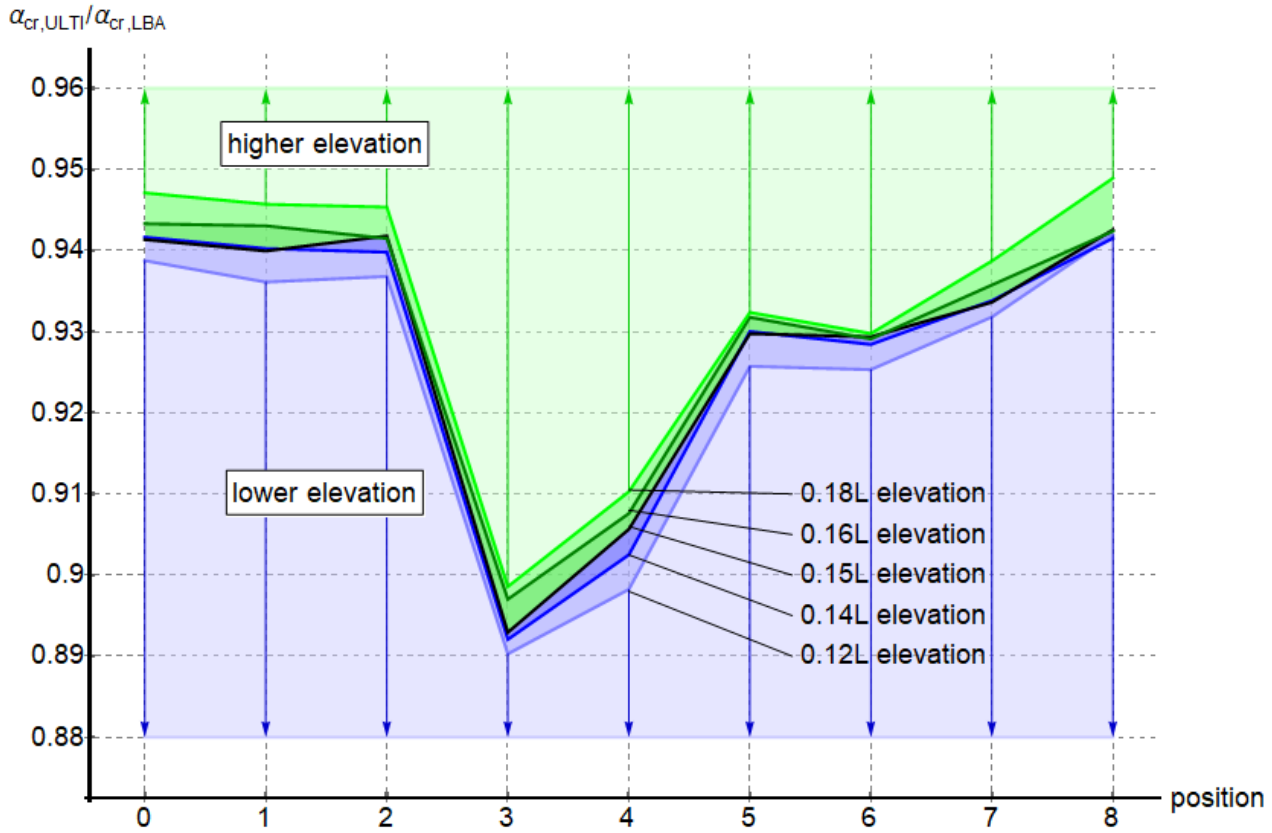


Figure 19: Ranges of ULTI-to-LBA critical load factor ratios for various elevations and predicted trends.

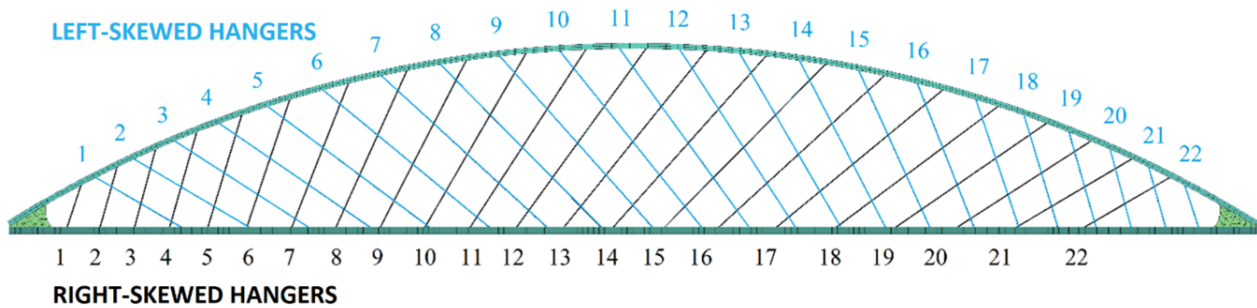


Figure 20: The numeration scheme of hangers' arrangement.

single and two following cables in the deck is considered with no tension and no prestress. Nine positions of live load are considered for every hanger rupture. A numeration scheme of hangers' arrangement is presented in Fig. 20.

In case of breaking one hanger at once, the resultant range of critical load factor ratios for both right- and left-skewed hangers changes from 0.6 to 0.9 (Fig. 21). Values fluctuate mainly nearby skewbacks and remain constant in midspan vicinity in the range from 0.7 to 0.8.

Furthermore, the left part of the right-skewed hangers' graph is symmetrical to the right part of the left-skewed hangers' graph toward the midspan.

In the event of rupturing two closest hangers (Fig. 22), the resultant range of critical load factor ratios changes from 0.725 to 0.875 (Fig. 23). Again, the values fluctuate mostly nearby skewbacks, but the range of changes is smaller than for rupturing one hanger case. In a specific accidental case, the farther the distance between the

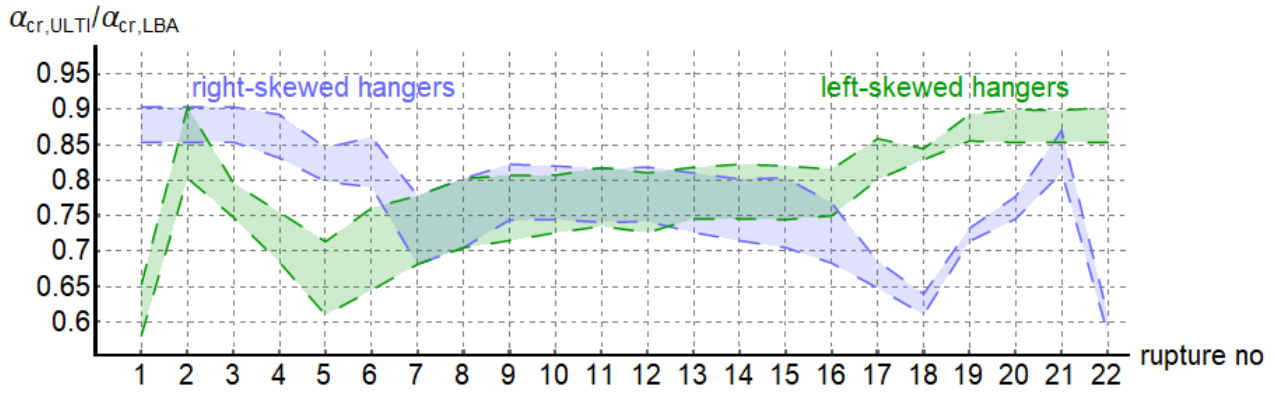


Figure 21: The range of ULTI-to-LBA critical load factor ratios for breaking one hanger at once.

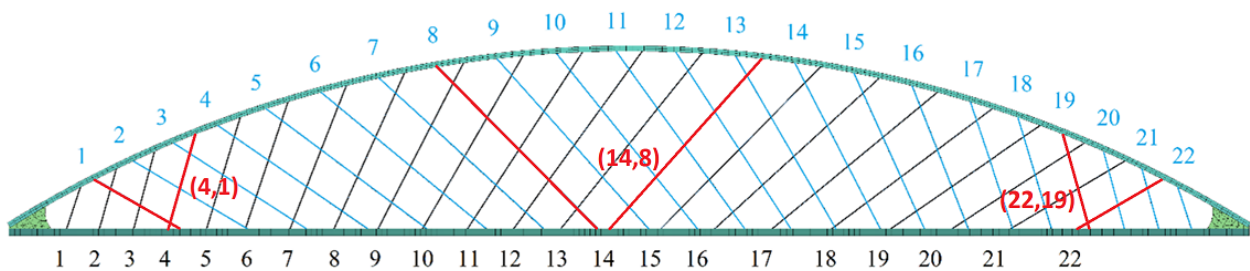


Figure 22: Examples of rupturing two nearest hangers.

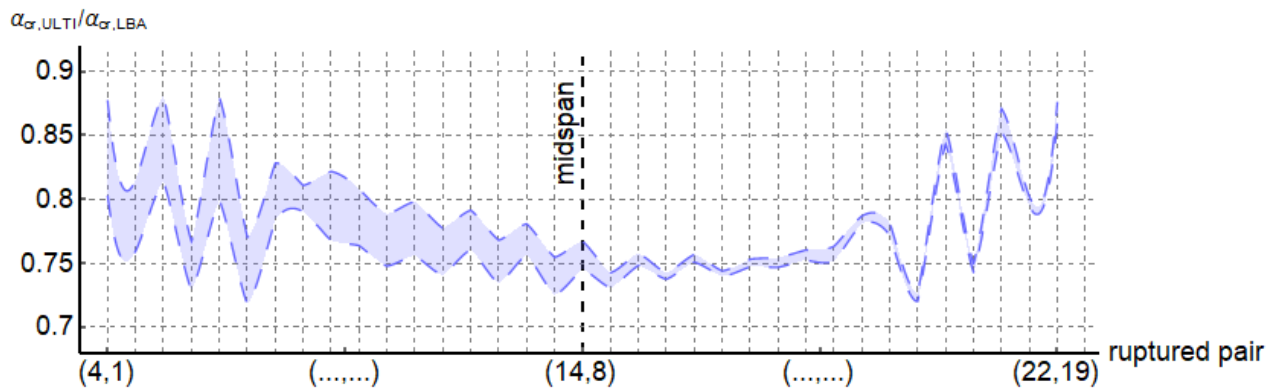


Figure 23: The range of ULTI-to-LBA critical load factor ratios for breaking two nearest hangers at once. The first number in brackets on the horizontal axis corresponds to the right-skewed hanger and the second number to the left-skewed hanger.

applied loads and ruptured hangers is, the wider the range of ratios gets, which is caused by the local phenomenon. Values remain approximately 0.75 in the midspan.

To compare instability shapes from the LBA and TH3 analysis, the most unfavorable load case position is considered for three specific hanger ruptures: nearby skewback, in one-fourth of the span, and in the midspan (Fig. 24). These analyses demonstrate the sensitivity to

failure of a single hanger. Instability deformations are similar for hangers' rupture in one-fourth and half of the span, but the axes of TH3 buckled forms are under the initial axis of the arch, when the LBA forms are symmetrical to the initial axis of arch. In the case of rupturing the closest hanger to the skewback, the LBA form is unaffected and deformed mainly in the midspan, when the TH3 form deforms mostly nearby this rupture.

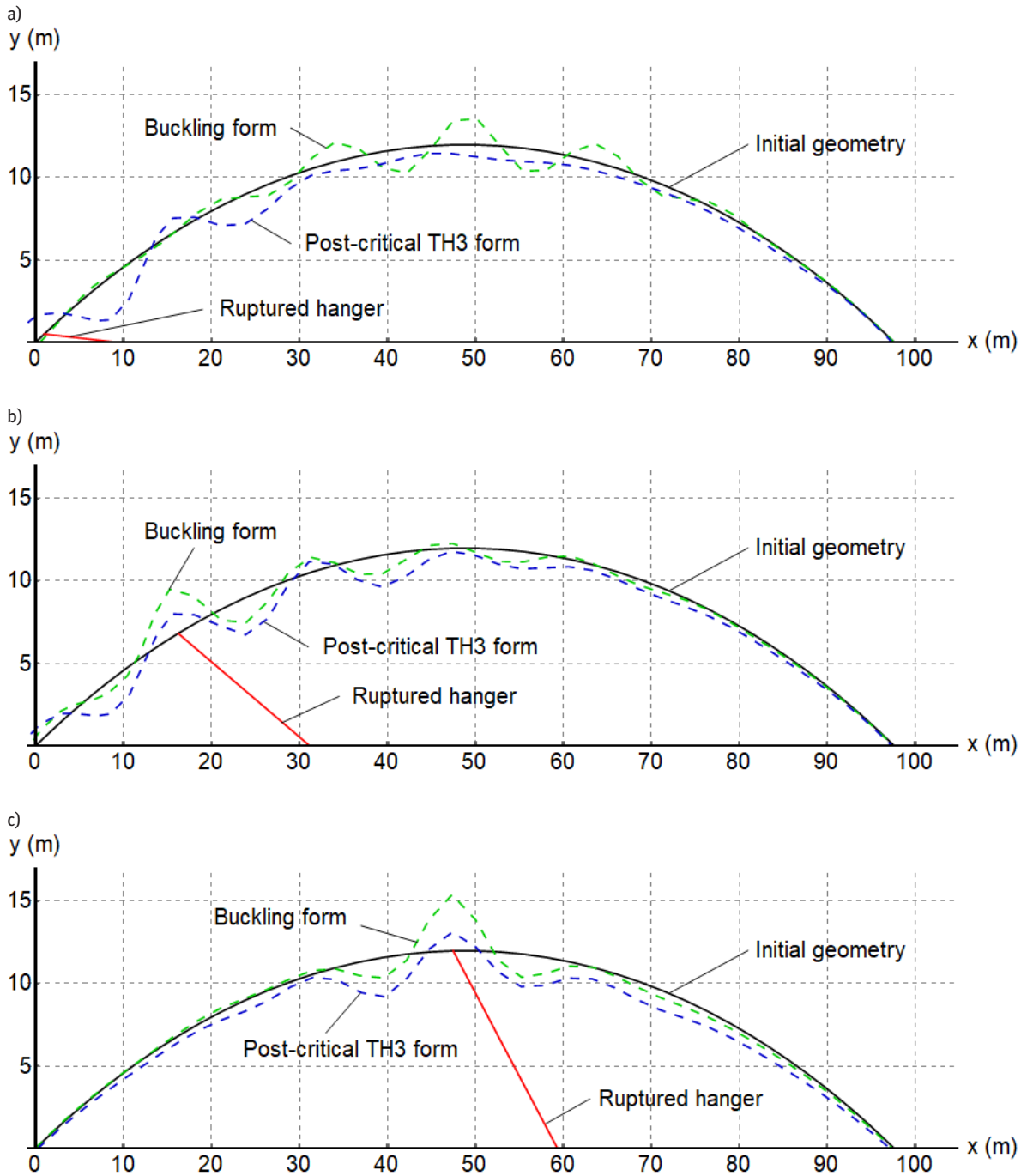


Figure 24: Scaled, exemplified deformations of instability forms of the arch between skewbacks from LBA and TH3 analysis: rupturing the leftmost hanger (a), rupturing the hanger in one-fourth of the span (b), and rupturing the hanger in the midspan (c).

5 Conclusions

The comparison of the critical load factor for geometrical LBA and non-LBA is conducted to investigate the influence of nonlinear phenomena. The proposed techniques are based on identification of the critical load factor from gradually incremented loads in the TH3 analysis. It

provides an opportunity to take into account the nonlinear behavior of cables, which cannot be obtained in the LBA. As a result, these nonlinear effects lead to divergencies in critical load factor values and shapes of imperfection forms in comparison to linear analysis.

In the considered range of values, prestress causes negligible impact on the nonlinear critical load factor.

On the other hand, greater tensile forces result in bigger differences between linear and nonlinear critical load factors. Since the nonlinear factor is always lesser than the linear factor (when prestressing and tensioning are applied in LBA analysis), this tendency can reflect in greater utilization of the arch. In the situation with all hangers without prestress and tension, the critical load ratio reaches values ranging between 0.89 and 0.94. In accidental case, when one hanger is ruptured at once, this range drops to 0.58–0.9. These values fluctuate mainly nearby skewback and stabilize in the midspan. The same tendency occurs when the two nearest hangers rupture (from the deck point of view); however, the range reduces to 0.74–0.88. Nevertheless, the change of range has a tendency to gradually decrease in the midspan from approximately 0.94 for no rupture case through 0.74–0.82 for one hanger break to 0.74–0.77 for two hanger breaks. This decline is greater between breaking one and no hanger and lesser between breaking two and one hanger. The change of range fluctuates less in the midspan. In the reasonable range of arch elevation, the ratio of critical loads is approximately 1% divergent from base 0.15 elevation and reaches values between 0.89 and 0.95. In cases with all cables, the greatest differences between linear and nonlinear critical load factor values manifest close to one-fourth of the span, which is correlated with the most unfavorable load position for arch structures.

Differences between the LBA and the TH3 buckled forms depend on the distribution of hangers, their tensioning, and eventually their failure, as presented. The additional deformations occur nearby skewbacks in the TH3 analysis compared to the LBA. Besides these regions, instability forms indicate similar tendencies, but TH3 form axes are always under the initial arch axis (similar to bow deformation) when LBA axes match it exactly. A new method for determining imperfection form for the arch bridges is proposed to establish nonlinear buckling form by subtracting some precritical deformations from the post-critical state. The resultant form is then a combination of the bow and the sinusoidal imperfection. The first one is similar in form point of view to those proposed in Eurocode [18]. The second one is a multi-period sinus shape, when the second imperfection in Eurocode [18] is only a single period. The amplitude of the bow and the sinus imperfections should be calculated based on the UGLI procedure using the nonlinear critical load factor value. Because of lesser values of the critical load factor, higher utilization of the arches' cross section is expected. For the reason of simplification, as an engineering approach, forms from the LBA and the load factor from the ULTI may be implemented in the UGLI procedure. The

simplification is mostly related to negligible sinusoidal deformations nearby skewback in the LBA; the closer the vehicle load is applied to skewback, the more significant the deformations are. Comparison of results of these procedures will be done in the next step.

Even though the optimal system of tensing hangers is not under consideration, it is found that additional tension above the forces resulting from self-tensioning (caused by deck weight) decreases the value of the critical load factor. Further studies are needed to determine the possibility of obtaining appropriate distribution of forces in hangers without additional external tensile force.

Data Availability Statements: All data and models generated or used during the study appear in the submitted article.

References

- [1] Graße, W., P. Tveit, S. Teich. 2003. "Calculation of a double track railway network arch bridge applying the European standards." Accessed May 20, 2021. https://home.uia.no/pert/data/Masters%20theses/diplom_brunn_schanack.pdf
- [2] da Costa, B. M. 2013. "Design and Analysis of a Network Arch Bridge." Master Thesis. Instituto Superior Tecnico. University of Lisbon. Portugal: Lisbon
- [3] Lorenc, W., T. Kaczmarek, T. Galewski, K. Topolewicz, R. Sęk, A. Radziecki, W. Ochojski, M. Kożuch. 2020. "Network arch bridges using cold-bent HD profiles: the Polish experiences." *Ernst & Sohn Verlag für Architektur und technische Wissenschaften GmbH & Co. KG*. <http://dx.doi.org/10.1002/stco.202000034>
- [4] Outtier, A., K. Schotte, H. de Backer, D. Stael. 2010. "Design Methods for Buckling of Steel Tied Arch Bridges." *IABSE Symposium Report*
- [5] Pipinato, A. 2018. "Structural Optimization of Network Arch Bridges with Hollow Tubular Arches and Chords." *Modern Applied Science*, vol. 12, no. 2
- [6] Rykaluk, K. 2012. "Zagadnienia stateczności konstrukcji metalowych" [Steel structures instability issue]. [In Polish.] *Dolnośląskie Wydawnictwo Edukacyjne*
- [7] Sęk, R., K. Szewczyk, B. Pilujski, D. Sobala, W. Lorenc, M. Kożuch. 2020. "Bridge over vistula river in cracow: the first railway network arch bridge using cold-bent HD sections and composite dowels." *IABSE*
- [8] Tveit, P. 2011. "The Network Arch. Finding on network arches during 54 years." Accessed May 20, 2021. <https://home.uia.no/pert/data/The%20Network%20Arch%2019-08-2014.pdf>
- [9] Tveit, P. 2014. "The Network Arch, bits of manuscript in march 2014 after lectures in 50+ countries." Accessed May 20, 2021. <https://home.uia.no/pert/data/The%20Network%20Arch%2019-08-2014.pdf>
- [10] Tveit, P., B. Brunn, M. Chan, W. Graße, F. Millanes, M. Ortega, R. Presland, R. Lee, L. Sasek, F. Schanack, P. Steere,

- G. Wollmann, T. Zoli. 2014. "Systematic Thesis on Network Arches." Accessed May 20, 2021. <https://home.uia.no/pert/data/Systematic%20Thesis%20on%20Network%20Arches%2009-09-14.pdf>
- [11] Tveit, P. 2011. "About the network arch, second edition." Accessed May 20, 2021. <https://home.uia.no/pert/data/About%20the%20network%20arch.pdf>
- [12] Tveit, P. 2014. "Efficient Utilisation of Optimal Network Arches." Agder University. Norway: Kristiansand. Accessed May 20, 2021. <https://home.uia.no/pert/data/Efficient%20Utilisation%20of%20Optimal%20Network%20Arches.pdf>
- [13] Tveit, P. 2009. "Genesis and development of the network arch concept." Accessed May 20, 2021. https://home.uia.no/pert/data/Genesis%20and%20Development%20of%20the%20Network%20Arch%20Concept_NY.pdf
- [14] Tveit, P. 2012. "On network arches for architects and planners." Lecture given at NTNU in Trondheim. Accessed May 20, 2021. <https://home.uia.no/pert/data/On%20Network%20Arches%20for%20Architects%20and%20planners25-10-14.pdf>
- [15] Timoshenko, S. P., J. N. Goodier. 2010. "Theory of elastic stability." Third edition. Mc Graw Hill. India
- [16] Zienkiewicz, O. C., R. L. Taylor. 2005. "The finite element method for solid and structural mechanics." Sixth edition. Elsevier. UK
- [17] CEN (European Committee for Standardization). 2005. *Design of steel structures. Part 1-1: General rules and rules for buildings*. Eurocode 3, Brussels, Belgium: CEN
- [18] CEN (European Committee for Standardization). 2009. *Design of steel structures. Part 2: Steel bridges*. Eurocode 3, Brussels, Belgium: CEN
- [19] CEN (European Committee for Standardization). 2003. *Actions on structures. Part 2: Traffic loads on bridges*. Eurocode 3, Brussels, Belgium: CEN